Polymer Vol. 39 No. 25, pp. 6589–6596, 1998

0032-3861/98/$ - see front matter

PII: S0032-3861(97)10171-9

The characterisation of random propylene–ethylene copolymer

Y. Feng and J. N. Hay*
The School of Metallurgy and Materials, The University of Birmingham, Edgbaston, Birmingham B15 2TT, UK
(Revised 26 September 1997)

The comonomer sequence distribution of a propylene–ethylene random copolymer has been investigated by a combination of temperature rising elution fractionation, ^{13}C nuclear magnetic resonance spectroscopy, Fourier transform infrared spectroscopy and differential scanning calorimetry (d.s.c.). The propylene–ethylene copolymer exhibited a wide range of comonomer compositional heterogeneity and there were no detectable long ethylene sequences containing three or more adjacent ethylene units in any of the fractions. The copolymer was mainly composed of long propylene sequences with an occasional ethylene unit. Sequences such as PPE, EPE, and PEP were present. The sequence distributions of all the fractions did not fit either Bernoullian or first order Markovian statistics. The ethylene content and the comonomer distribution had a marked effect on the crystallisation kinetics and melting behaviour of the fractions.

(Keywords: propylene–ethylene random copolymer; comonomer sequence distribution; temperature rising elusion fractionation)

INTRODUCTION

The properties of polyolefin copolymers are dependent on morphology, degree of crystallinity and lamellae size distribution and vary markedly with comonomer composition and sequence distribution, rather than molecular weight distribution. Copolymers prepared by heterogeneous catalysts often exhibit compositional heterogeneity since it is generally accepted that these catalysts have a plurality of active species[1–4]. In particular, propylene–ethylene random copolymers produced by such systems contain a range of copolymers with different composition and sequence distribution[5,6]. Many analytical techniques have been employed to measure their compositional heterogeneity including gel permeation chromatography, column fractionation[7] and successive Soxhlet extraction using different solvents[8].

Temperature rising elution fractionation (TREF) has been successfully applied to the fractionation[9–11] of a number of ethylene copolymer systems, such as linear low density polyethylenes, and has proved to be a more effective method than successive Soxhlet extraction, since the temperature range for fractionation can be chosen more freely to match solubility. More importantly, the interpretation of TREF data is more straightforward, as temperature is the only main variable during the fractionation. TREF has in particular been shown to be a powerful technique for the studies of compositional heterogeneity of polyolefins[9,12–14].

In the present paper we report on the comonomer composition and sequence distribution of a random propylene–ethylene copolymer using TREF over a wide temperature range. The fractions obtained by TREF were characterised by ^{13}C n.m.r. and also *FT*i.r. spectroscopy. The crystallisation and melting behaviour of these fractions have been investigated.

* To whom correspondence should be addressed

EXPERIMENTAL

A random propylene–ethylene copolymer sample, RPE, was obtained from Solvay—grade number KV202—and the ethylene content was about 5 mol%. Fractionations were carried out on about 1 g of sample dissolved in 400 cm^3 of xylene at 130°C, stabilised with the antioxidant Santanox R. Solutions were loaded directly on to the top of a TREF column of packed finely divided silica sand at 130°C. The column was slow cooled overnight to room temperature, resulting in a progressive deposit of the copolymer on to the top third of the column. The first fractions were eluted at room temperature by passing xylene through the column, and represented unprecipitated material. Consecutive fractions were obtained by increasing the elution temperature stepwise to 125°C, each temperature step being selected to produce fractions of approximately equal weight. In order to achieve equilibrium elution, the column was kept at each temperature for 45 min before elution was continued at a higher temperature. The eluted fractions were precipitated into a large excess of methanol at room temperature, filtered and dried in a vacuum oven at 60°C to constant weight.

^{13}C Nuclear magnetic resonance spectra, (^{13}C n.m.r.) were measured at 130°C on a 270 MHz Jeol GX270 Fourier Transform ^{13}C n.m.r. spectrometer. 10 wt vol% of polymer solutions were prepared in *o*-dichlorobenzene with 5% deuterated DMSO as an internal lock.

Fourier transform infrared (*FT* i.r.) spectra were measured on a Mattson Polaris Spectrometer, interfaced to a PCV computer on compression moulded films 10~100 μm thick.

A Perkin–Elmer differential scanning calorimeter, DSC-2, interfaced to a BBC-Master computer via an analogue to digital converter, was used to characterize the thermal properties of the fractions. The temperature scale of the d.s.c. was calibrated from the melting points of zone refined stearic acid (m.p. 343.5 K) and high purified metals such as

Table 1 Fractionation of the PE random copolymer

Fraction number	Elution temp (°C)	Weight (mg)	ω_i (%)	$C(M_i)$
R1	18	0.0 ± 0.1	0.00	0.00
R2	40	0.6	0.06	0.03
R3	60	1.9	0.19	0.16
R4	80	116.2	11.78	6.14
R5	90	132.7	13.45	18.76
R6	95	147.7	14.97	32.97
R7	100	160.4	16.25	48.34
R8	102	100.8	10.21	61.81
R9	105	95.0	9.63	71.73
R10	107	86.2	8.74	80.91
R11	110	79.4	8.05	89.31
R12	112	25.6	2.59	94.63
R13	115	30.0	3.04	97.44
R14	117	9.4	0.95	99.44
R15	120	0.0	0.00	99.91
R16	123	0.9	0.09	99.96

Weight of samples used: 1.20 g

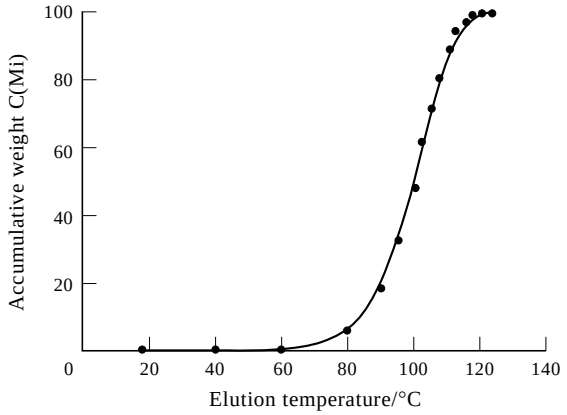

Figure 1 Accumulative weight–elution temperature of the copolymer

indium (m.p. 429.78 K), tin (m.p. 505.06 K), lead (m.p. 600.50 K), and zinc (m.p. 692.65 K). The thermal response of the calorimeter was calibrated from the heat of fusion of ultra pure indium, taken to be 28.4 J g^{-1}. Samples were encapsulated in aluminium pans and an empty aluminium pan was used as reference.

RESULTS AND DISCUSSION

Fractionation and characterisation

16–20 fractions were obtained in each TREF fractionation and a typical analysis of fractional weight against elution temperature is given in *Table 1*. Schulz's method[15] of plotting the accumulative weight fraction, $C(M)$, against elution temperature was adopted, such that for the ith fraction of weight ω_i,

$$C(M_i) = \frac{1}{2}\omega_i + \sum_{i-1}^{j=1} \omega_j \qquad (1)$$

An average accumulative weight–elution temperature distribution curve determined is shown in *Figure 1*. It can be seen that the random copolymer fractions precipitated over a wide temperature range, from 60 to 120°C

The fractions were analysed by ^{13}C n.m.r. spectroscopy since it has been shown[16–18] to be a powerful technique for characterising the detailed molecular structure of copolymer chains, and it is sensitive to monomer sequencing and compositional variations. *Table 2* lists the chemical shifts

Table 2 Chemical shifts and peak assignments in propylene–ethylene copolymer

	Chemical shifts (ppm)	
Assignments	Calculated	Measured
$S_{\alpha\alpha}$–C_H2	46.4	45.5
$S_{\alpha\gamma}$–CH_2	37.9	36.8
$S_{\alpha\delta}$–CH_2	37.5	36.5
$S_{\alpha\beta}$–CH_2	34.5	–
$T_{\delta\delta}$–EPE–CH	33.2	33.0
$T_{\beta\delta}$–EPP–CH	30.9	31.5
$S_{\gamma\gamma}$–CH_2	30.7	31.0
$S_{\gamma\delta}$–CH_2	30.4	29.5
$S_{\delta\delta}$–CH_2	30.0	29.0
$T_{\beta\beta}$–PPP–CH	28.5	28.0
$S_{\beta\gamma}$–CH_2	27.8	–
$S_{\beta\delta}$–CH_2	27.4	26.5
$S_{\beta\beta}$–CH_2	24.7	23.5
$P_{\beta\beta}$ CH_3–mmPPP	21.8	21.0
CH_3–mγPPP		
$P_{\beta\delta}$ CH_3–PPE	20.9	20.5
CH_3–$\gamma\gamma\gamma$PPP		
$P_{\delta\delta}$ CH_3–EPE	20.7	19.8

calculated and measured for the different carbon atoms in the copolymer chains adopting the nomenclature of Carman[16], for which a methylene carbon is identified as S with two Greek letters indicating its distance in both directions to the nearest tertiary carbons such that the letter δ indicates the methylene is 3C away from a tertiary carbon. Similarly, a methine carbon is identified as T with two Greek letters showing the positions of the nearest tertiary carbons. A methyl carbon is given the letter P with two Greek letters which are the same as those for the attached tertiary carbon.

The intensity of each peak in the ^{13}C n.m.r. spectra was used to calculate the sequence content of the comonomers. The dyad concentrations were determined from the methylenes data using[19]:

$$PP = S_{\alpha\alpha}$$

$$EP = S_{\alpha\gamma} + S_{\alpha\delta}$$

$$EE = \tfrac{1}{2}(S_{\beta\delta} + S_{\delta\delta}) + \tfrac{1}{4}S_{\gamma\delta}$$

The triad concentrations were analysed from both methine and methylene data using,

$$PPP = T_{\beta\beta}$$

$$PPE = T_{\beta\delta}$$

$$EPE = T_{\delta\delta}$$

$$PEP = S_{\beta\beta} = \tfrac{1}{2}S_{\alpha\gamma}$$

$$EEP = S_{\alpha\delta} = S_{\beta\delta}$$

$$EEE = \tfrac{1}{2}S_{\delta\delta} + \tfrac{1}{4}S_{\gamma\delta}$$

The monomer compositions were calculated from both the dyad and triad concentrations from the equations:

$$P = PP + \tfrac{1}{2}PE$$

$$E = EE + \tfrac{1}{2}PE$$

$$P = PPP + PPE + EPE$$

$$E = EEE + EEP + PEP$$

Figure 2 shows the variation of propylene and ethylene content of the TREF fractions as measured by n.m.r.

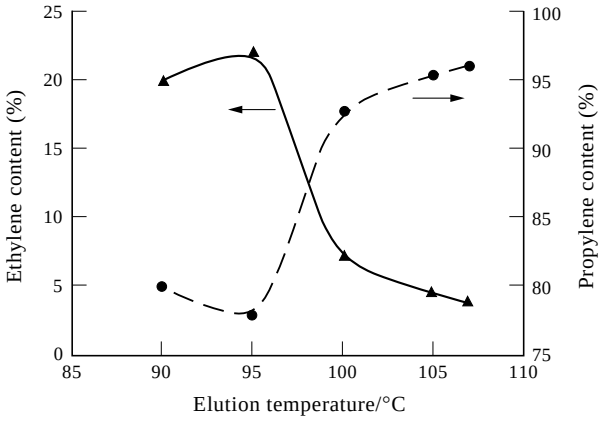

Figure 2 Variation of the propylene and ethylene content with elution temperature

spectroscopy with elution temperature. *Table 3* lists the dyad and triad concentrations of each fraction. It is apparent that TREF is fractionating by comonomer composition since the propylene content increases and ethylene content decreases with increasing elution temperature. For comparison, the corresponding dyad and triad concentrations calculated from Bernoullian and first order Markovian statistical models[19] are also given.

The content of long ethylene sequences in the fractions containing more than three E units, EEE, is virtually zero. The dyad ethylene, EE, content is also relatively low and it decreases with increasing elution temperature. The fractions are essentially composed of long propylene sequences with some isolated ethylene units, such as PPE, EPE, and PEP. With increasing eluting temperature, the content of isolated E units also decreases in that above 105°C the fractions consist essentially of long sequences of P units interspersed with isolated E units. This is readily seen from comparison of the sequence distributions of fractions, R5 and R10, produced at 90 and 107°C respectively. The propylene dyads increase from 0.668 to 0.925, the triads from 0.580 to 0.892 while, on the other hand, the ethylene sequences *[EE]* decrease from 0.066 to 0.010. Since the ethylene co-units decreases, the *[PPE]* decreases from 0.167 to 0.061 as well as *[EPE]* from 0.056 to 0.007, the *[PEP]* from 0.066 to 0.020 and the *[EEP]* from 0.133 to 0.033.

The number average sequence length were derived from:

$$\overline{n_P} = \frac{[PP] + \frac{1}{2}[PE]}{\frac{1}{2}[PE]}$$

$$\overline{n_E} = \frac{[EE] + \frac{1}{2}[PE]}{\frac{1}{2}[PE]}$$

For comparison the Bernoullian model, gives the following relationships

$$n_A = 1/(1 - P_A),\ n_B = 1/P_A \quad (6)$$

and the first-order Markovian model,

$$n_A = 1/P_{AB},\ n_B = 1/P_{BA} \quad (7)$$

where n_A and n_B are the number average sequence length of comonomer A and B; P_A, P_B, the probability of forming a sequence with monomer with A or B as an active centre, and P_{AB} and P_{BA} are conditional probability of forming a chain with an active centre as AB* or BA*.

Table 3 Sequence distribution

Sequence	Observed value	Bernoullian model	Markovian model
(a) Sequence distribution of the copolymer fractions			
Fraction R5			
E	0.199	–	0.262
P	0.801	–	0.738
PP	0.668	0.642	0.528
EP	0.265	0.319	0.419
EE	0.066	0.040	0.052
PPP	0.580	0.514	0.378
PPE	0.167	0.255	0.300
EPE	0.056	0.032	0.060
PEP	0.066	0.128	0.168
EEP	0.133	0.063	0.084
EEE	~0	0.008	0.010
Fraction R6			
E	0.220	–	0.290
P	0.780	–	0.710
PP	0.618	0.608	0.469
EP	0.318	0.343	0.483
EE	0.064	0.048	0.048
PPP	0.600	0.475	0.309
PPE	0.103	0.268	0.319
EPE	0.077	0.038	0.082
PEP	0.096	0.134	0.201
EEP	0.127	0.076	0.081
EEE	~0	0.011	0.008
(b) Sequence distribution in the fractions			
Fraction R7			
E	0.072	–	0.108
P	0.928	–	0.892
PP	0.882	0.861	0.809
EP	0.091	0.134	0.166
EE	0.027	0.005	0.025
PPP	0.879	0.799	0.734
PPE	0.026	0.124	0.151
EPE	0.023	0.005	0.008
PEP	0.037	0.062	0.064
EEP	0.017	0.010	0.038
EEE	0.018	0.000	0.006
Fraction R9			
E	0.046	–	0.071
P	0.954	–	0.929
PP	0.924	0.910	0.873
EP	0.059	0.088	0.111
EE	0.016	0.002	0.015
PPP	0.852	0.868	0.821
PPE	0.069	0.084	0.105
EPE	0.033	0.002	0.003
PEP	0.027	0.042	0.044
EEP	0.005	0.004	0.024
EEE	0.014	0.000	0.003
(c) Sequence distribution in the fractions			
Fraction R10			
E	0.039	–	0.076
P	0.961	–	0.924
PP	0.925	0.924	0.863
EP	0.065	0.075	0.122
EE	0.010	0.002	0.015
PPP	0.892	0.888	0.806
PPE	0.061	0.072	0.114
EPE	0.007	0.001	0.004
PEP	0.020	0.036	0.049
EEP	0.033	0.003	0.024
EEE	~0	0.000	0.003

The number average sequences of P and E comonomer units are tabulated in *Table 4*. from which it is apparent that in all the fractions the average ethylene sequence length is very short (about 1.5), corresponding to isolated E or EE units on average. The propylene sequence lengths, however, increases markedly. Neither the first order Markovian nor the Bernoullian statistical model were appropriate descriptions for these sequences distributions and no distinction

Table 4 Number-average ethylene and propylene sequence lengths in the fractions and a comparison with the statistical models

Fractions	Measured values		Bernoullian model		Markovian model	
	n_E	n_P	n_E	n_P	n_E	n_P
R5	1.50	6.04	1.248	5.03	1.25	3.52
R6	1.40	4.89	1.282	4.55	1.20	2.94
R7	1.54	32.32	1.048	21.70	1.27	16.67
R9	1.40	20.38	1.078	13.89	1.30	10.75
R10	1.31	29.46	1.041	25.64	1.25	15.15

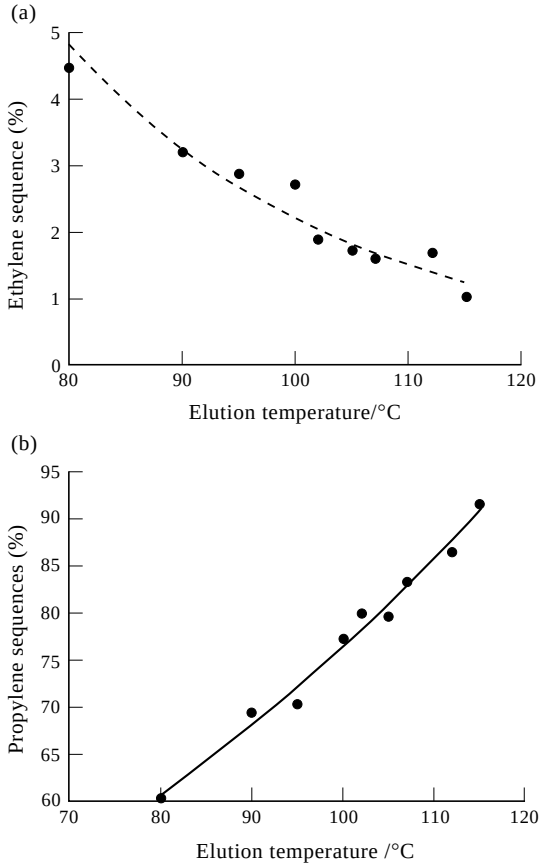

Figure 3 Variation of the ethylene sequence content with elution temperature; variation of propylene dyads with elution temperature

could be made between them. In particular, the Bernoullian was a better description of the ethylene sequence distribution and that it was essentially constant with comonomer content while the first order Markovian was is better in describing the propylene sequences dependence on composition.

An attempt was made also to estimate the ability of *FT* i.r. spectroscopy to measure these comonomer distributions. The absorption band at 722 cm^{-1} is characteristic[20] of the rocking vibration of methylene sequences, $(CH_2)_n$ for $n > 3$, and the absorption at 722 cm^{-1} was taken to be a measure of longer ethylene sequences, EEE. *Figure 3* shows the change in the absorption with eluting temperature, from which it is apparent that content was decreasing with elution temperature, in an analogous manner to that observed in the n.m.r. analysis.

Two absorption bands at 998 and 973 cm^{-1} were used to characterise the propylene content. Ciampelli and

Table 5 Propylene and ethylene dyad content

Fractions	EE		PP	
	^{13}C n.m.r.	*FT*i.r.	^{13}C n.m.r.	*FT*i.r.
R5	6.6	3.2	66.8	69.4
R6	6.4	2..9	61.8	70.3
R7	2.7	2.7	88.2	77.1
R9	1.6	1.7	92.4	79.4
R10	1.0	1.6	92.5	83.0

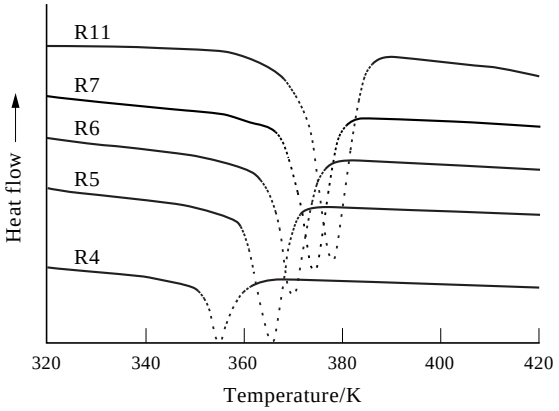

Figure 4 DSC crystallisation curves for the copolymer fractions

Valvassori[21] have suggested that the latter is characteristic of a CH_3 group isolated from other CH_3 groups by several CH_2 units, and that the band at 998 cm^{-1} is characteristic of CH_3 groups separated by only one methylene group. Theoretical calculations performed by Zerbi[22] also indicate that the 973 cm^{-1} band is characteristic of isolated propylene units and it has been tested by examining the IR spectra of various hydrocarbons with methyl branching[23]. It is evident that the position of such a band in a propylene–ethylene copolymer depends on the separation of the methyl groups along the copolymer chain. The relative absorbance of the band at 998 cm^{-1} was considered to be proportional to the number of propylene units present in sequences of two or more propylene units and that at 973 cm^{-1} to be proportional to the number of isolated propylene units. The ratio between the absorbances at 998 and 973 cm^{-1}, therefore, gives an indication of the distribution of the propylene units in propylene–ethylene copolymers. *Figure 3* shows this variation in the fractions with elution temperature. The PP sequences increase monotonously with increasing eluting temperature, and thus the TREF was separating the fractions according to their propylene content. The propylene and ethylene dyad sequences of the fraction obtained by ^{13}C n.m.r. and *FT* i.r. spectroscopy are not identical but are comparable, see *Table 5* Both analytical techniques are not identical but nevertheless they are in accordance with one another.

The development of crystallinity in the fractions

The temperature range over which crystallisation occurred in the fractions was investigated on cooling from the melt at a standard rate of 10 K min^{-1}. The range over which crystallinity developed and broadened, and the initial onset temperature, decreased progressively with increasing ethylene content, see *Figure 4*. Observations on subsequent melting, see *Figure 5*, indicated that the polypropylene

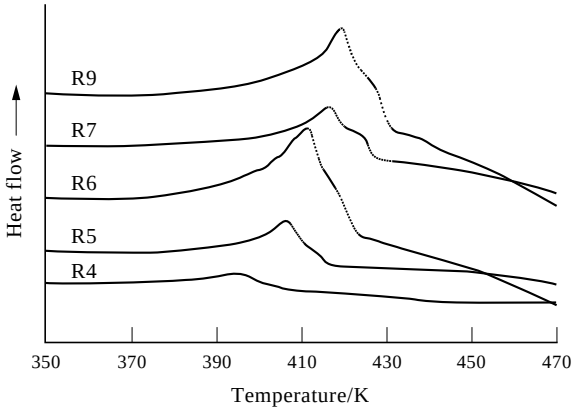

Figure 5 DSC melting behaviour of the fractions

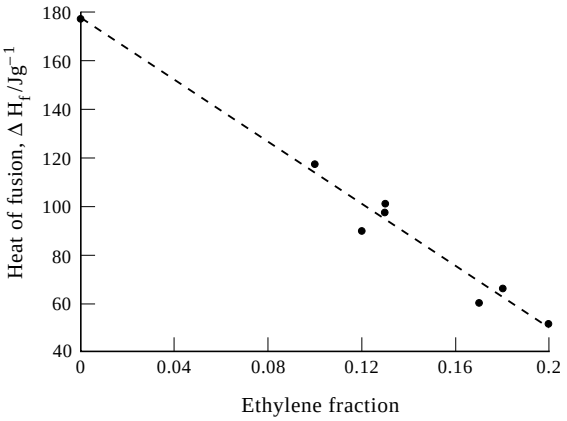

Figure 6 Effect of ethylene content on heat of fusion

groups only had crystallised and that the degree of crystallinity which developed in the fractions, as measured from the observed heats of fusion decreased linearly with the increase in the ethylene content, see *Figure 6*. It is apparent that isolated ethylene units alone are sufficient to inhibit the development of crystallinity in the copolymer by being partially excluded into the amorphous regions. The extrapolated heat of fusion for the isotactic polypropylene was about 180 J g^{-1} i.e. 7.9 kJ mol^{-1}.

Differential scanning calorimetry was also used to measure the isothermal crystallisation of the fractions from the rate of heat evolution with time, following the procedures adopted previously[24,25]. A comparison of the crystallisation behaviour of polyethylene, as measured by d.s.c. and dilatometry, showed that d.s.c. gave just as meaningful kinetic data as dilatometry, but the technique was more convenient to use.

Samples were melted at 470 K for 10 min to destroy any crystals which may still be present in the sample, cooled to the crystallisation temperature (T_c) at 160 K min^{-1} and cooling and the crystallisation exotherm recorded until the calorimeter response returned to the baseline. The initial heat loss by the sample during cooling to the crystallisation temperature, T_c, was subtracted and the isothermal crystallisation curves analysed.

Assuming that the heat evolved is due to crystallisation, then the fractional extent of crystallinity, $X(t)$, can be evaluated by integrating the exotherm from the start to time, t, i.e.

$$X(t) = \int_0^t \frac{dH}{dt} d \Big/ \int_0^\infty \frac{dH}{dt} dt \qquad (8)$$

The fractional extent of crystallinity with time was analysed by the Avrami equation, for which

$$-\ln(1 - X_t) = Zt^n \qquad (9)$$

The presence of both primary and secondary crystallisation processes, with correspondingly different exponent values, were observed for each fraction. The Avrami exponent n of the primary crystallisation process was determined as a function of conversion by differentiating the above equation with respect to time, such that

$$n = -t\frac{dX'_t}{dt} \Big/ \left[\ln\left(\frac{1}{1 - X'_t}\right)(1 - X'_T)\right] \qquad (10)$$

where X'_t refers to the fractional crystallinity at the end of the primary crystallisation process.

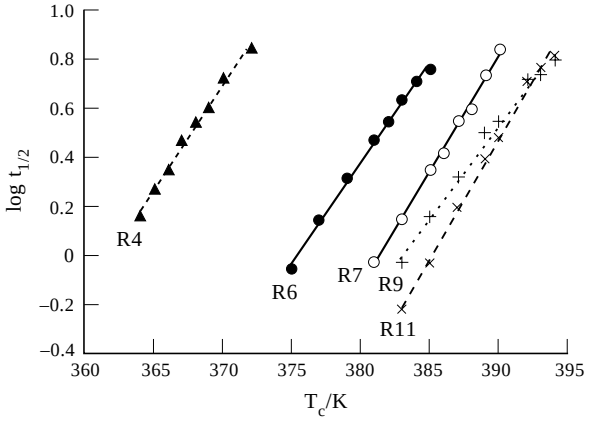

Figure 7 The variation of the crystallisation half-life with temperature

The composite rate constant, Z was then determined from the half life of the primary process, $t_{1/2}$, such that,

$$Z = \ln(2)/(t_{1/2})n \qquad (11)$$

The crystallization rates, as measured by the half lives, $t_{1/2}$, of the isothermal crystallisation of the fractions are markedly temperature-dependent, the rate doubling for each 1 K temperature rise. Fractions with increasing ethylene content crystallised at similar rates at progressively lower temperatures, see *Figure 7*, the difference between the temperature at which each fraction crystallized at similar rates being as much as 25 K. Again it is apparent that the presence of the ethylene comonomer inhibited the development of crystallinity.

The variation of the Avrami parameter, n, with the dyad EE sequence content is shown in *Figure 8*. The exponent, n, decreased from about 3.0 for polypropylene consistent with the growth of predetermined spherulites to values below 2.0—decreasing with increasing EE content. A similar decrease has been observed with comonomer content in other copolymer systems and has been attributed to non-crystallisable comonomer units being rejected by the growing crystals. There is thus a clear indication that the ethylene hinders crystal growth and produces an open textured spherulite with the incorporation of increasing amounts of non-crystallisable materials within the spherulite boundaries.

The melting point of the copolymers

Figure 5 shows the d.s.c. melting curves of the various fractions. The equilibrium melting temperatures of each of

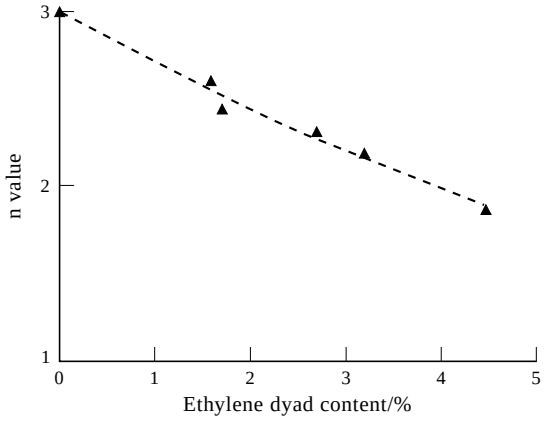

Figure 8 The effect of ethylene dyad content on the Avrami exponent, *n*

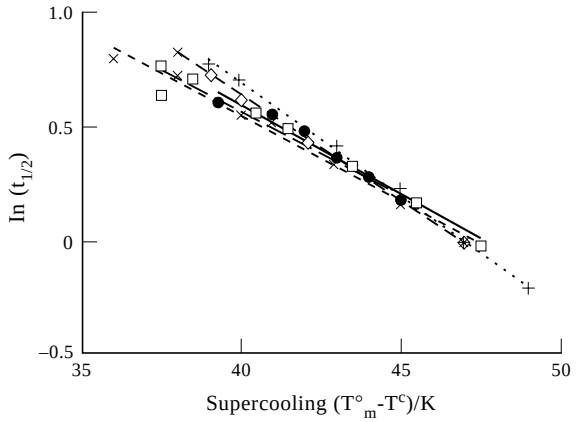

Figure 9 The dependence of the crystallisation half-lives on the degree of supercooling

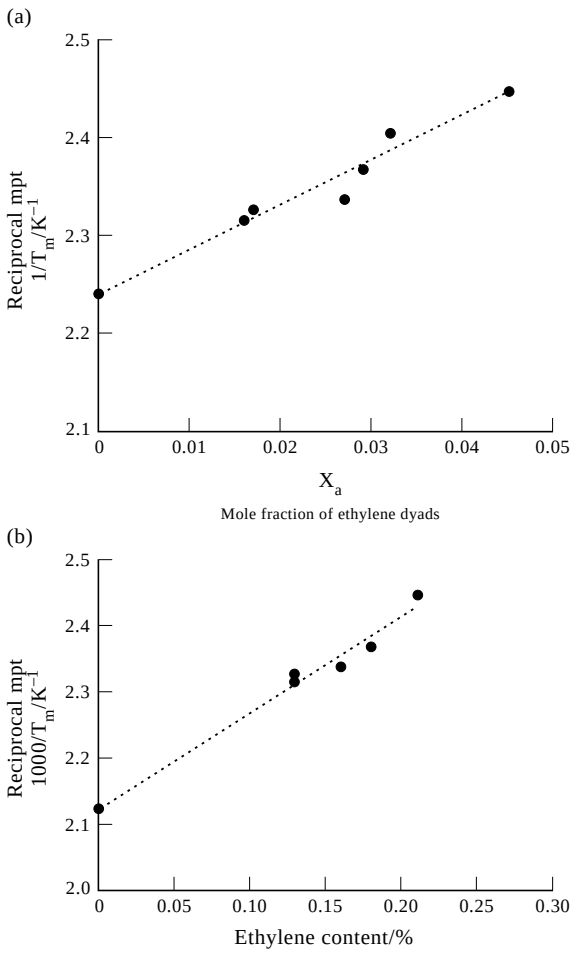

Figure 10 Depression of m.p. by ethylene dyads; depressions of the equilibrium m.p. by ethylene units

the fractions T_m^0 were evaluated by the Hoffman–Weeks method[27] of plotting the observed m.p., T_m against the crystallization temperature, T_c. The fractions were observed to melt exhibiting multiple melting peaks and the observed m.p. was defined by the temperature corresponding to the last trace of crystallinity. This did not change by more than 1 K over an increase in the crystallization temperature of 10 K. This observed change is much smaller than that allowed by the Hoffman–Weeks treatment and was attributed to improvement in crystal perfection at the higher crystallisation temperatures. The m.p.s did not correspond to the expected behaviour for nucleation control of the crystal thickness which is inherent in the Hoffman–Weeks treatment but are characteristic of crystals whose thicknesses are limited by sequence length limitations. M.p.s were accordingly limited by comonomer content rather than the size of the critical size nucleus. Correspondingly, since only the long propylene sequences could crystallise, increasing the ethylene content of the fraction reduced these on the average and so reduce the crystallinity which could develop, see *Figure 6*. The observed m.p.s of the fractions at their higher crystallization temperatures are listed in *Table 7* and an extreme variation of 23 K was observed between the m.p.s of the fractions. This was consistent with the large differences observed in the temperature range over which the various fractions crystallised, see *Figure 5*. Indeed, the plots of $\ln(t_{1/2})$ against crystallisation temperature, T_c, see *Figure 7* were essentially superposed when plotted against the degree of supercooling, $(T_m - T_c)$, see *Figure 9*, implying that the rate of crystallisation was controlled by the depression of the m.p.

Flory[33] using an equilibrium crystallisation model related the equilibrium melting point of a copolymer to composition, by:

$$1/T_m - 1/T_m^0 = -(R/\Delta H_f)\ln(x_b) \qquad (13)$$

where x_a is the mole fraction of crystallisable units in the copolymer,

For small values of x_b, this reduces to:

$$1/T_m - 1/T_m^0 = (R/\Delta H_f)(x_a)$$

where x_a represents is the mole fractions of non-crystallisable units.

The question remains as to what is the non-crystallisable rejected comonomer unit—an isolated E, or a dyad, EE or higher sequence? Plots of $1/T_m^0$ for each fraction against x_a where x_a was in turn the concentration of E and EE units present in the fraction were linear, see *Figure 10*. Using the dyad as the rejected group, the intercept corresponded with a T_m^0 of 445 ± 2 K and a heat of fusion of 1.84 ± 0.05 kJ mol^{-1} for isotactic PP compared with 459 K and 8.79 kJ mol^{-1} conventionally quoted for these values The values are clearly wrong. If the Flory relationship is at all valid for this copolymer system then clearly the ethylene dyad is not the unit which inhibits crystallisation. The impurity unit is present in greater concentrations than the

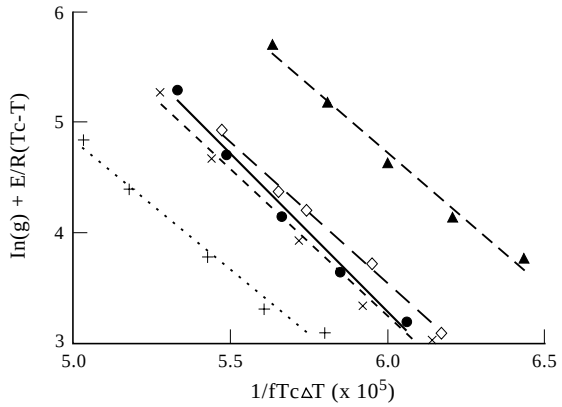

Figure 11 The temperature-dependence of the crystallisation growth rate

Table 6 Crystallographic unit cell dimensions for polypropylene[28]

(110) Growth plane	
a_0 (m):	5.49×10^{-10}
b_0 (m):	6.26×10^{-10}
$(a_0 b_0)$ (m^2):	3.43×10^{-19}

dyad. Using isolated E units alone, a value of 460 ± 5 K was determined for the equilibrium m.p. of polypropylene and the heat of fusion was 7.5 ± 0.5 kJ mol^{-1}. This is more consistent with the accepted values for these parameters and implies that an isolated E unit alone is acting as the rejected impurity group in lowering the m.p. and inhibiting the crystallisation of the random copolymers.

Temperature-dependence of crystallization rate

The growth rate data was analysed by the Lauritzen–Hoffman[26] treatment in order to determine the effect of ethylene in changing the free energy of the fold surface of the lamellae. Accordingly, the growth rate g, is

$$g = g_o \exp[-\Delta E/R(T_c - T_g + 30)] \exp[-K_g/(f\ T_c \Delta T)] \quad (12)$$

where g_o is a constant, ΔE is the activation energy associated with the glass-forming process, ΔT is the degree of supercooling from the equilibrium m.p., R is the gas constant, T_g is the glass transition temperature and K_g is a nucleation constant.

$$f = 2T_c/(T_c + T_m^0)$$

By using $g = (t_{1/2})^{-1}$ which assumes that the nucleation densities and growth rates have the same temperature dependence and can be averaged and by rearranging equation (12), then

$$\ln(g) + \frac{\Delta E}{R(T_c - T_\infty)} = \ln(g_0) - \frac{K_g}{f\,T_c \Delta T} \quad (13a)$$

Using a standard value for DE of 6280 J mol^{-1} and 269.6 K[28] for the glass transition temperature of isotactic polypropylene plots of $[\ln(g) + \Delta E/R(T_c - T_\infty)]$ against $1/f\,T_c(\Delta T)f$ were linear, see *Figure 11*. From the slope of these lines the free energy of the fold surface, σ_e, were determined for each fraction. In this analysis and by comparison with references[29–31], it was assumed that all the crystallisations were carried out in Regime III, so that,

$$K_g = 4b_0 \sigma \sigma_e T_m^0/(\Delta H_f) K \quad (16)$$

Table 7 Variation of m.p. and surface free energy with ethylene content

Sample	E Content (%)	EE content (%)	T_m^0 (K)	K_g ($\times 10^{-5}$) (K^2)	σ_e (J m^{-2})
R4	21	4.5	409	2.846	0.0733
R5	18	3.2	423	2.627	0.0658
R7	16	2.7	428	2.554	0.0631
R9	13	1.7	430	2.443	0.0598
R11	13	1.6	432	2.319	0.0565

and

$$\sigma = \alpha (a_0 b_0)^{1/2} \Delta H_f$$

α has been derived empirically to be 0.1, from the Thomas–Stavely relationship[32]. The material constants for polypropylene used in the analysis are listed in *Table 6* and the kinetic parameters for the fractions are listed in *Table 7*. In general the free energy of the fold surface, σ_e, did not change substantially with increasing ethylene content in the copolymer due presumably to the rejected ethylene units on the fold surface being less sterically hindered than the propylene units and so not increasing the surface energy.

CONCLUSIONS

A propylene–ethylene random copolymer was fractionated by the TREF technique based on the comonomer content and crystallinity of each component in bulk polymer. The experimental results showed that the copolymer exhibits a wide variation in comonomer composition.

Isolated comonomer, dyad and triad concentrations in the copolymer were measured by ^{13}C n.m.r. spectroscopy from which it was evident that there were little or no long ethylene sequences containing more than two ethylene units present in the copolymers. All the fractions were composed of long propylene sequence interspaced with isolated ethylene comonomer units, such as, PPE, EPE, and PEP. As expected from the statistical nature of the copolymer the length of the propylene sequences increased with increasing elution temperature. The number-average of the ethylene sequences was very low, typically 1.5 and relatively constant-independent of ethylene content. This was consistent with the random characteristic of the copolymerization. However, neither a first-order Markovian nor the Bernoullian model were appropriate descriptions for either the propylene or ethylene sequences. The *FT* i.r. spectroscopic measurement of the dyad sequences—both for propylene and ethylene—were in broad agreement with the n.m.r. spectroscopic analysis.

Isothermal crystallisation rate studies and melting behaviour of the fractions were investigated as a function of ethylene content. The equilibrium melting point, T_m^0, decreased with increasing E content consistent with the isolated E unit disrupting the crystallisation of the propylene sequences. All the rate data were interpretable in terms of the equilibrium m.p. being depressed by isolated ethylene units, and the depression of T_m^0 was in agreement with the Flory's equation. The free energy of the fold surface was not greatly altered by the presence of the ethylene content which was not unexpected since these units are unlikely to increase steric hindrance of a hydrocarbon chain compared to the propylene unit. The effect of the ethylene unit in the crystallisation of the copolymer is primarily that of depressing the m.p. of the polypropylene crystals.

ACKNOWLEDGEMENTS

Y. Feng is pleased to acknowledge the award of a research grant from the Sino–British Friendship Scholarship Scheme during the tenure of this work.

REFERENCES

1. Cozewith, C. and Ver Strate, G., *Macromolecules*, 1971, **4**, 482.
2. Boor, J. *Ziegler–Natta Catalysis and Polymerisations*. Academic Press, New York, 1979.
3. Vizen, Y. I. and Yakobson, F. I., *Polymer Science USSR (Engl. Transl.)*, 1979, **20**, 1046.
4. Kissen, Y. V., *Isospecific Polymerisation of Olefins with Heterogeneous Ziegler–Natta Catalysts*. Springer, New York, 1985.
5. Kakugo, M., Naito, Y., Mizunuma, K. and Miyatake, T., *Macromolecules*, 1982, **15**, 1150.
6. Hayashi, T., Inoue, Y. and Chujo, R., *Macromolecules*, 1988, **21**, 3139.
7. Riess, G. and Callot, P., in *Fractionation of Synthetic Polymers*, ed. L. H. Tung. Marcel Dekker, New York, 1977.
8. Saga, K., Shiono, T. and Doi, Y., *Makromolecules Chemistry*, 1988, **189**, 1531.
9. Zhou, X. Q. and Hay, J. N., *European Polymer Journal*, 1993, **29**, 291.
10. Wild, L., *Advances in Polymer Science*, 1990, **98**, 1.
11. Glockner, G. J., *Applied Polymer Science Applied Polymer Symposium*, 1990, **45**, 1.
12. Nakano, S. and Goto, Y. J., *Applied Polymer Science*, 1981, **26**, 4217.
13. Usami, T., Gotoh, Y. and Takayama, S., *Macromolecules*, 1986, **19**, 2322.
14. Kakugo, M., Naito, Y., Mizunuma, K. and Miyatake, T., *Makromolecules Chemistry*, 1989, **190**, 849.
15. Schulz, G. V., *Z. Physik. Chem.*, 1940, **B47**, 155.
16. Carman, C. J. and Wilkes, C. Z., *Rubber Chemical Technology*, 1971, **44**, 781.
17. Wilkes, C. Z., Carman, C. J. and Harrington, R. A., *Journal of Polymer Science (Physics)*, 1973, **43**, 237.
18. Carman, C. J. and Baranwal, K. C., *Rubber Chemical Technology*, 1975, **48**, 705.
19. Randall, J. C., *Polymer Sequence Determination (Carbon 13 NMR method)*. Academic Press, 1977.
20. Bucci, G. and Simonazzi, T., *Journal Polymer Science Part C*, 1964, **7**, 203.
21. Ciampelli, F. and Valvassori, A., *Journal Polymer Science Part C*, 1967, **16**, 377.
22. Zerbi, G., Gussoni, M. and Ciampelli, F., in *International Symposium on Macromolecular Chemistry*, Prague, 1965, Preprint No. 567.
23. Smith, D. C., US Naval Research Laboratory Report, C-3294.
24. Mills, P. J. and Hay, J. N., *Polymer*, 1982, **23**, 1380.
25. Booth, A. and Hay, J. N., *Polymer*, 1969, **10**, 95.
26. Lauritzen, J. I. Jr. and Hoffman, J. D., *Journal of Applied Physics*, 1973, **44**, 4340.
27. Hoffman, J. D. and Weeks, J. J., *Journal of Research in Natl. Bur. Std. A. Phys. Chem.*, 1962, **66A**(1), 13.
28. Janimak, J. J., Cheng, S. Z.D., Giusti, P. A. and Hsieh, E. T., *Macromolecules*, 1991, **24**, 2253.
29. Clark, E. J. and Hoffman, J. D., *Macromolecules*, 1984, **17**, 878.
30. Cheng, S. Z.D., Janimak, J. J., Zhang, A. and Cheng, H. N., *Macromolecules*, 1990, **23**, 298.
31. Goldfarb, L., *Makromol. Chem.*, 1978, **179**, 2297.
32. Thomas, D. G. and Stavely, L. A. K., *Journal of Chemistry Society*, 1952, 4569.
33. Flory, P. J., *Transactions of the Faraday Society*, 1955, **51**, 848.